A little case study of an offset-dependent seismic response

J. Helen Isaac and Don C. Lawton

ABSTRACT

A small baseline 3D3C seismic survey was acquired in May, 2014, at the Brooks Field Research Station (FRS) in Southern Alberta. This area is of interest for planned experimental CO_2 injection, initially into the Basal Belly River sandstone at 295 m. We created PP and PS synthetic seismograms from dipole sonic and density logs acquired in a well 8 km away to enable us to identify the reflectors seen on the processed seismic data, especially in the shallow zone of interest. Subsequently we derived a shear sonic log from a compressional sonic log to tie the seismic data with synthetic seismograms from a well at the FRS site.

The high amplitude positive response (peak) at the top of the Upper Cretaceous Milk River Formation sandstone on the default normal incidence synthetic seismogram does not match that of the PP seismic data, which has a weak response. The Zoeppritz equations predict a high amplitude reflection coefficient at zero-offset, a decrease in amplitude with increasing offset and a change in polarity at an incidence angle of 35°, or about 250 m, resulting in a low amplitude stacked response for this high impedance sandstone. The character of the Milk River reflection on the seismic data stacked with all offsets matches the stacked offset synthetic seismogram while the character of the Milk River reflection on the seismic data stacked with only the near offsets matches the normal incidence synthetic seismogram.

The seismic character of the PS data matches that of the PS synthetic seismogram.

INTRODUCTION

The Containment and Monitoring Institute (CaMI), part of Carbon Management Canada, has established a Field Research Station (FRS) for testing and calibrating various technologies for monitoring the behaviour of injected CO_2 and cap rock integrity (www.cmcghg.com/business-units/cami). The plan at the FRS is to inject small amounts (up to 1000 tonnes per year) of CO_2 into the subsurface. The primary injection target is the water-wet Upper Cretaceous Basal Belly River sandstone at 295 m, with a secondary target in the deeper Medicine Hat at 505 m. A possible later target is in the Second White Speckled Shale formation at 710 m.

SEISMIC DATA

A small baseline 3D3C seismic survey was acquired in 2014 over Section 22, T17 R 16W4M (Figure 1). The source was two Tesla Envirovibes at a source interval of 10 m along 17 lines spaced 100 m apart in an outer grid and 50 m apart in an inner grid. Receivers were also spaced at 10 m along 17 lines spaced 100 m and 50 m apart. Further details can be found in Lawton et al. (2014).

The processing and interpretation of the PP and PS data are discussed in Isaac and Lawton (2014 and this volume, respectively).

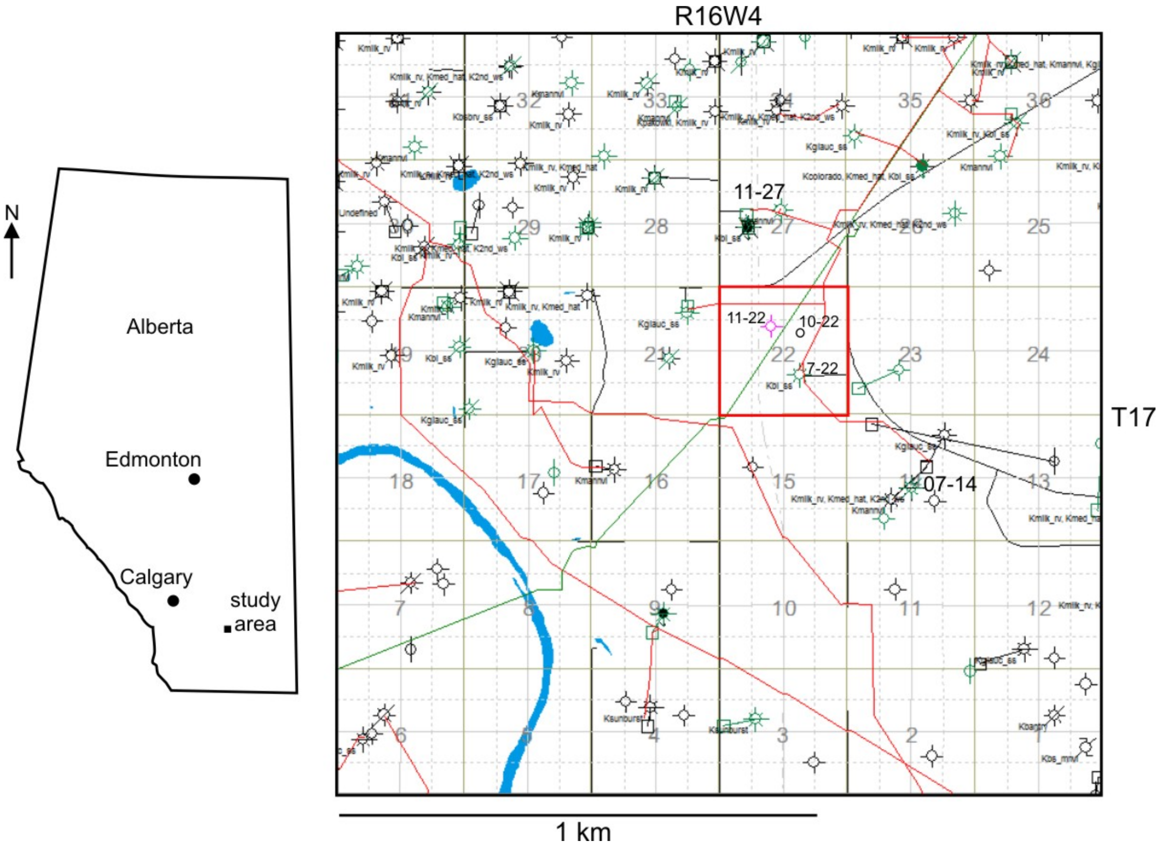

FIG. 1: The study area in Southern Alberta, with Section 22 highlighted in red. The annotations next to the wells show producing zones.

PP synthetic seismograms

We used GeoSyn software to create synthetic seismograms from the sonic and density logs obtained in well 07-22-017-16W4M to identify reflections on the seismic data (Figure 2). The correlation shows a good tie for the Basal Belly River reflection, and fairly good ties for the Medicine Hat, Base Fish Scales, Mannville and Ellerslie events. However, we observe a poor seismic character match between the seismic data and synthetic data at the top of the Milk River Formation (Figure 3), where the synthetic has a high amplitude peak and the seismic data have a weak peak. The sonic log shows a significant increase in velocity at the top of the Milk River Formation, which is a thin near-shore to terrestrial unit (Figure 4) at the top of the Colorado Group, the rest of which is predominantly a thick shale-dominated sequence. There are several possibilities for the cause of this mis-match: (1) the original sonic log was digitized incorrectly, (b) there is a problem with the processing of the seismic data, or (c) there is an issue with the synthetic seismogram.

We first investigated the original sonic log in case there was a scale change at the top of the Milk River that had been missed in the digitization. Figure 5 shows part of the original rastered sonic log. There is no scale change at or near the top of the Milk River Formation so we infer that the sonic log appears to have been digitized correctly. We also saw this deflection on sonic logs from other wells in the neighbourhood. Thus cause (a) was ruled out.

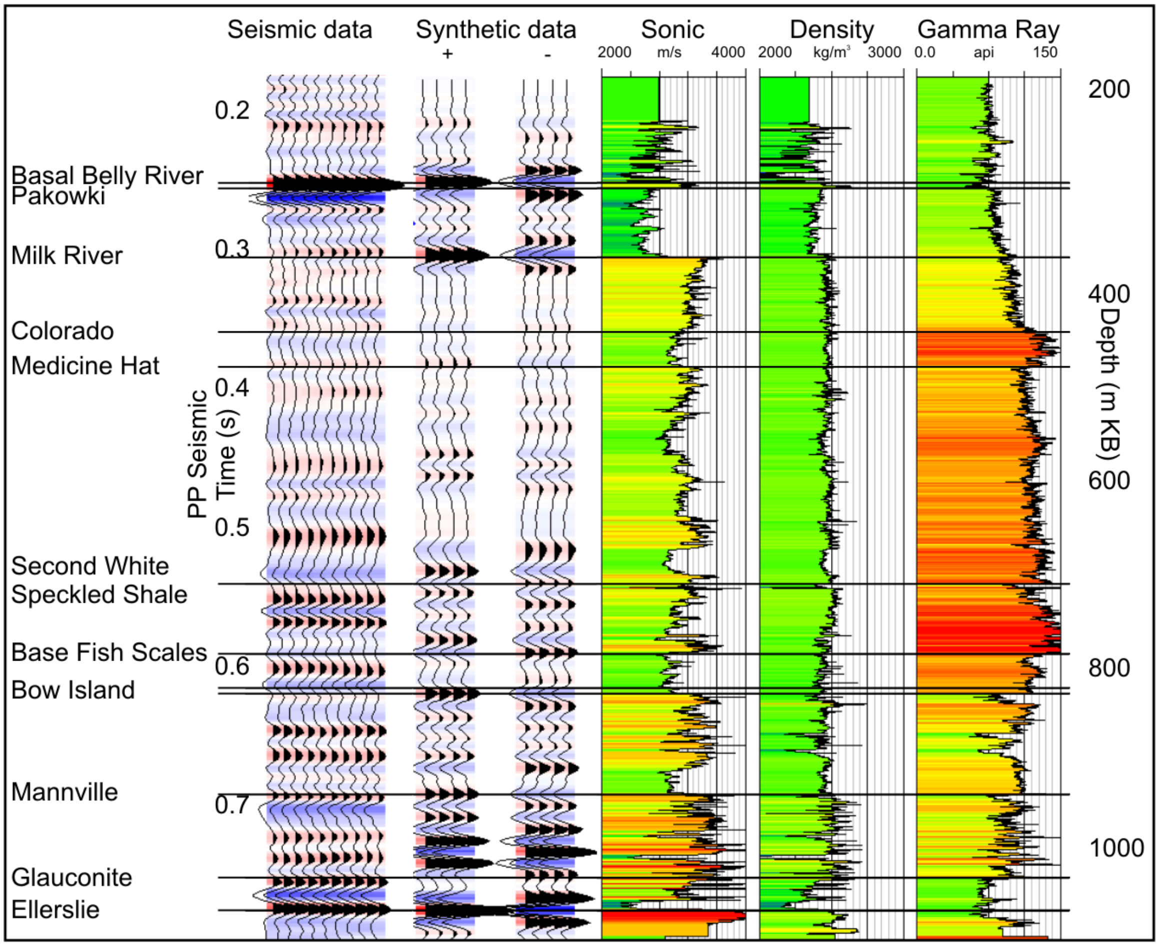

FIG. 2: Tie between seismic data and synthetic seismogram created from the sonic and density logs of well 07-22-017-16W4M.

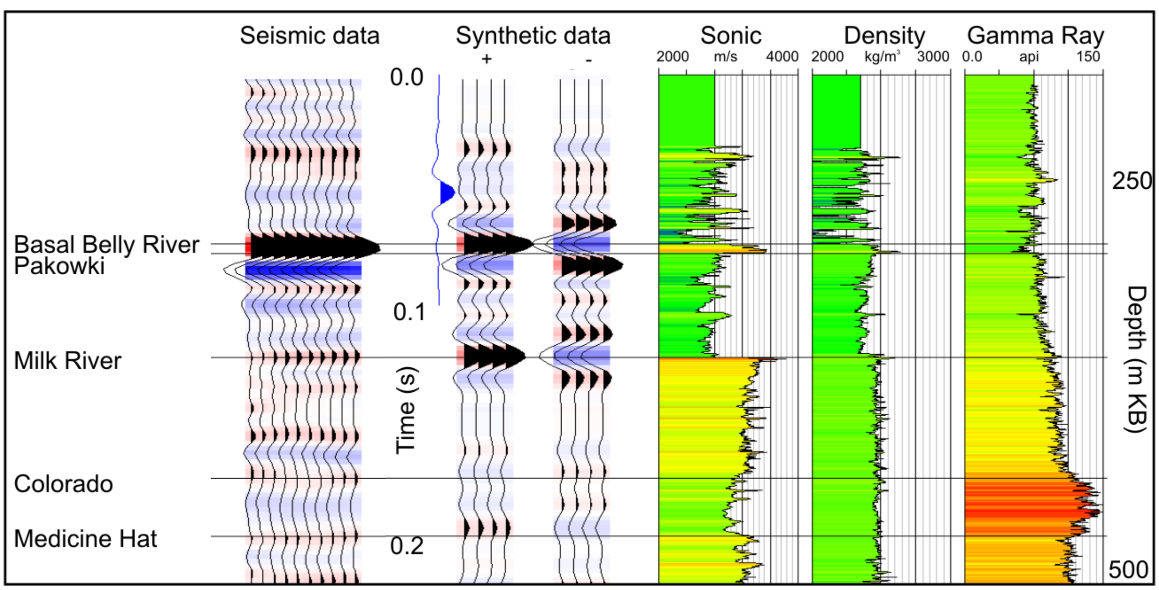

FIG. 3: Enlarged view of the tie between seismic data and the upper portion of the synthetic seismogram shown in Figure 2. There is clearly a character mis-match at the Milk River.

FIG. 4: Cliffs of the Milk River Formation in Southern Alberta.

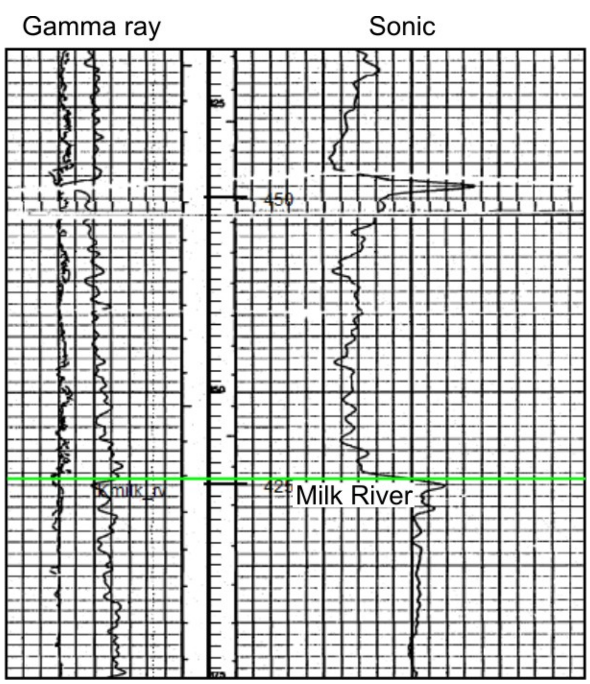

FIG. 5: Rastered sonic log from well 07-22-017-16W4M. There is no scale change at or near the top of the Milk River Formation so we believe that the sonic deflection to the right has been digitized correctly.

Cause (b), a problem with the processing of the seismic data, is one we would rather be incorrect as the processing seemed perfectly fine at the time, so let us move quickly to cause (c).

Our original tie (Figure 3) is between the seismic data and the default normal incidence synthetic seismogram. A more realistic simulation of the stacked multi-offset seismic data would be a stack of synthetic offset gathers. To create a multi-offset gather, a shear sonic log is needed but the well we are using here has no shear sonic log. However, a well drilled about 8 km away to the northeast, 01-07-018-15W4M, has a dipole log. We created an offset-dependent synthetic seismogram from the dipole compressional and shear logs of this well (Figure 6) using Aki and Richards' 2-term approximation (Aki and Richards, 1980) to the Zoeppritz equations (Zoeppritz, 1919). This seismogram shows a decrease in reflection coefficient amplitude with increasing offset at the top of the Milk River Formation. The reflection coefficient reverses polarity and the stacked offset gathers reveal a reflection with very low amplitude. This is an example of a Class 1 (Rutherford and Williams, 1989) or Type 1 (Young and LoPiccolo, 2003) AVO anomaly. This stacked synthetic response now correlates well to the character seen on the seismic data at the top of the Milk River Formation.

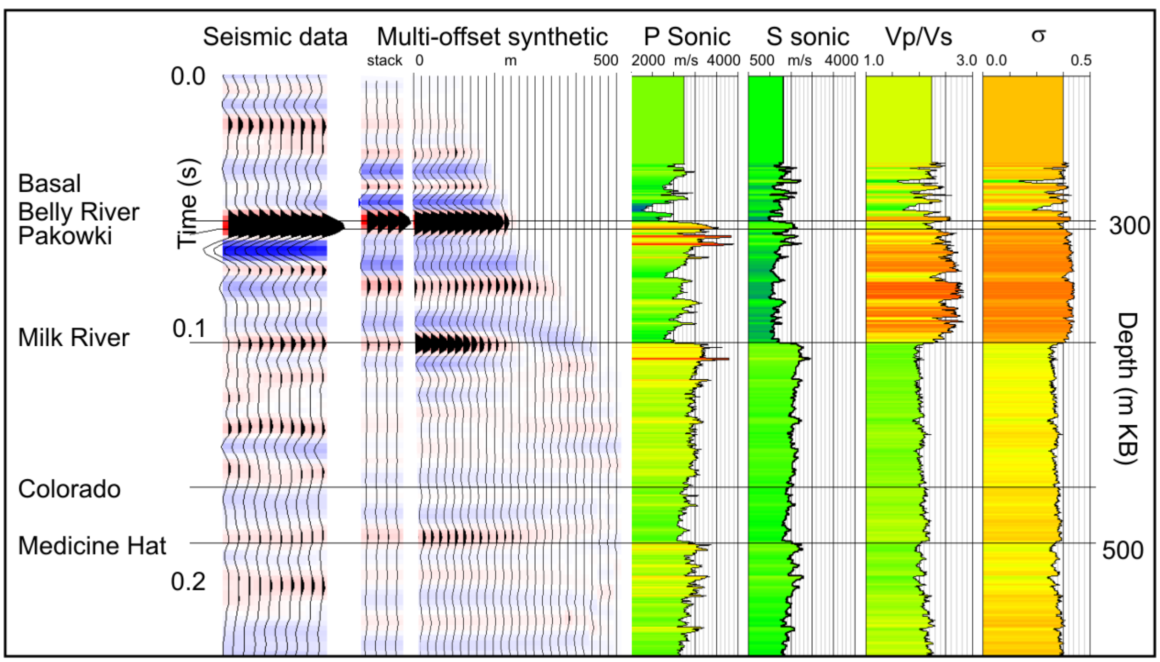

FIG. 6: Multi-offset synthetic seismogram created from the dipole logs recorded in well 01-07-018-15W4M, which is about 8 km away from the study area. The stacked response at the top of the Milk River Formation corresponds well to that seen on the seismic data.

Well 01-07-018-15W4M is about 8 km away from Section 22 and the formation thicknesses are a little different due to stratigraphic changes. Also there are character differences in the Pakowki-Milk River interval. Thus we desire to tie the seismic data to well 07-22-017-016W4M, which, however, does not have a shear sonic log. There are a few ways to create a shear sonic log. We might use the Vp/Vs values from 01-07-018-15W4M, either as calculated or blocked over intervals, then adjusted to match the formaton tops of 07-22-017-16W4M, use the shear sonic log from 01-07-018-15W4M, again either as is or blocked and adjusted, or derive a shear sonic log from the compressional sonic log using the Castagna mud rock relationship (Castagna et al., 1985). Using either of the first two ways would introduce the lithology of Section 7 into Section 22, and we know there are differences as we see them on the gamma ray logs. Using the mud-rock relationship we derived a shear sonic log from the compressional sonic log for well 01-07-018-15W4M. Figure 7 compares the measured shear log to the derived log and also shows the derived shear log for well 07-22-017-16W4M. Since the log derived using Castagna's equation for well 01-07-018-15W4M matches the measured log very well, especially close to the Pakowki/Milk River interface under investigation, we consider the derived shear log for well 07-22-017-16W4M to be valid for generating an offset synthetic seismogram.

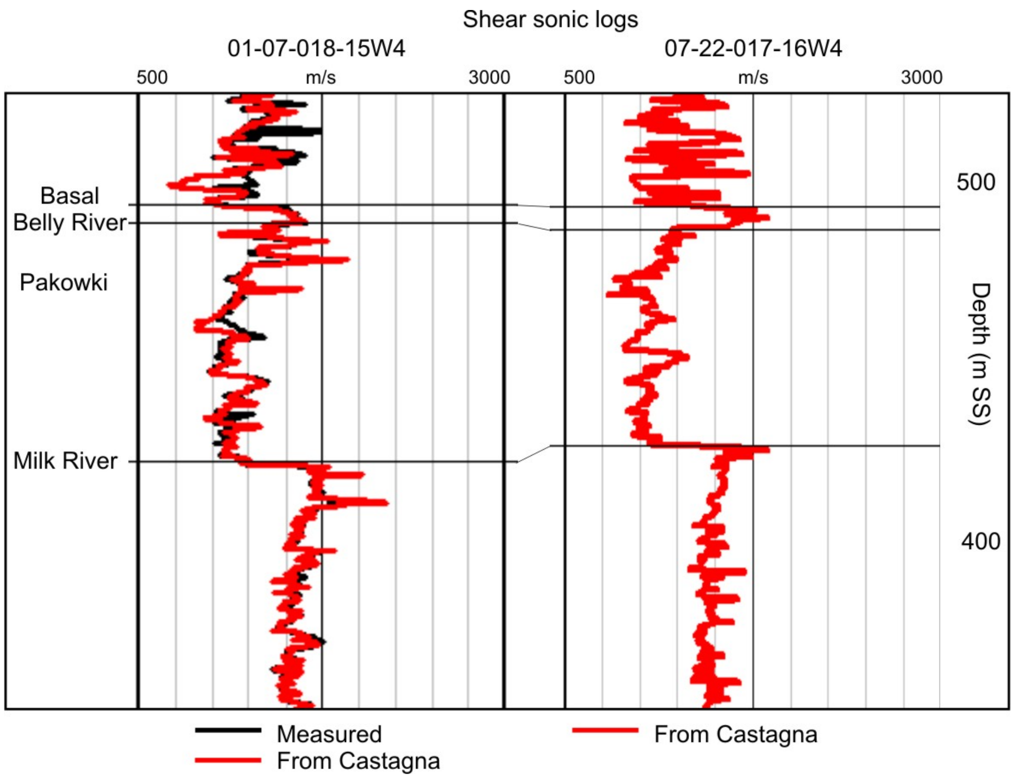

FIG. 7: Comparison of the measured shear sonic log and shear sonic derived from the compressional sonic log using Castagna's mud-rock equation for well 01-07-018-15W4M and the derived shear sonic log for well 07-22-017-16W4M.

Using this derived shear log we created the multi-offset synthetic seismogram displayed in Figure 8. The offset range used in the synthetic is comparable to the offsets present in the seismic data and the mute we applied to the gathers before stacking them was similar to that applied to the seismic data. We again see the reversal of polarity with offset at the top of the Milk River and the character of the Milk River event on the stacked synthetic matches the seismic data much better than that of the normal incidence synthetic in Figure 3.

We stacked the seismic data using limited offsets of 0-250 m to compare with the zero-offset synthetic seismogram. Figure 9 shows the same well tie as in Figure 3 but with part of the near offset migrated section replacing the section with all offsets. The character match between the seismic data and zero-offset synthetic data of the Milk River event is now much better.

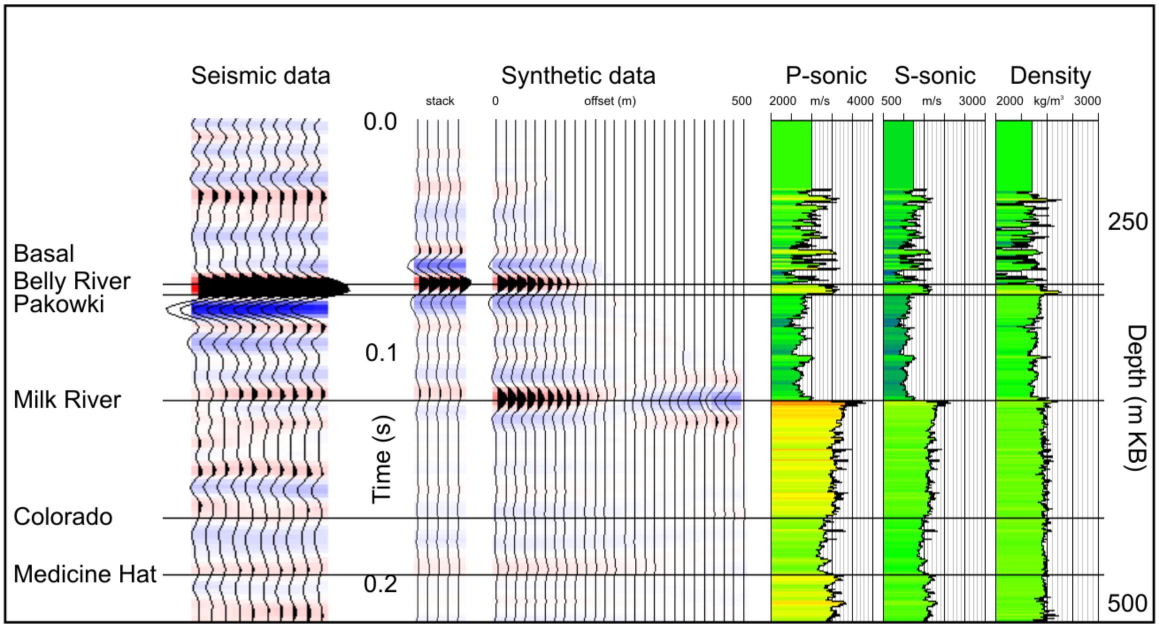

FIG. 8: Tie between seismic data and stacked multi-offset synthetic seismogram created from the compressional sonic and density logs and the derived shear sonic log of well 07-22-017-16W4M. The character match at the Milk River is much better than of the zero-offset synthetic seismogram in Figure 3.

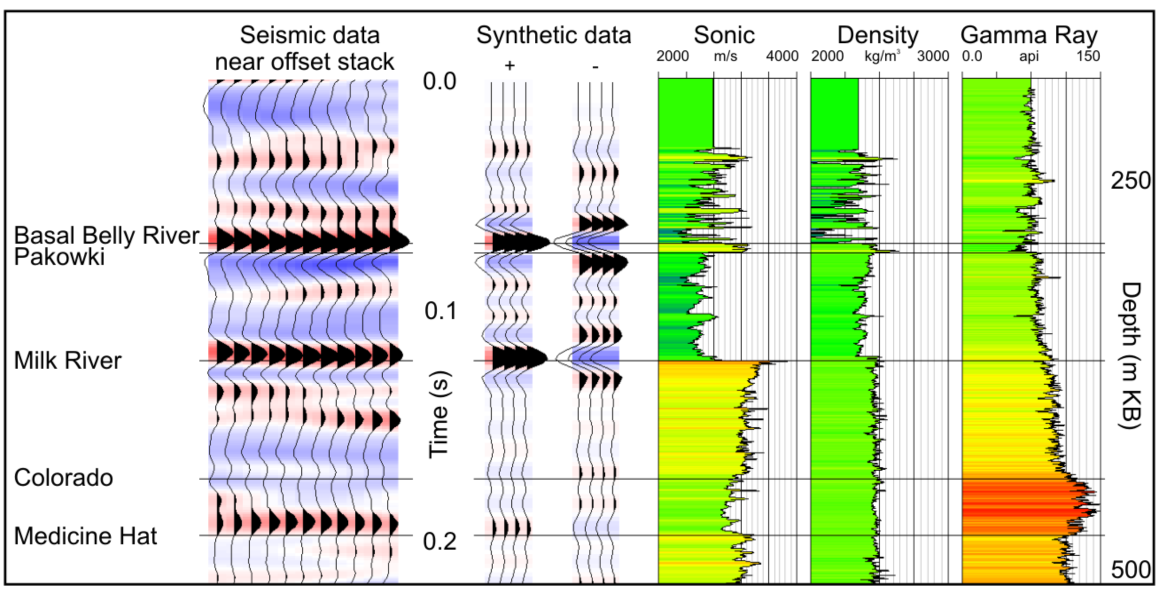

FIG. 9: Tie between near-offset (0-250 m) seismic data and synthetic seismogram created from the sonic and density logs of well 07-22-017-16W4M. The character match at the Milk River is much better than that of Figure 3, in which we used seismic data with all offsets.

This observed polarity reversal with offset could be predicted from the high impedance and the decrease in Poisson's ratio of the Milk River sandstone (Figure 6) since the Zoeppritz equations predict a decrease in amplitude with offset when impedance and Poisson's ratio change in different directions (Zoeppritz, 1919; Allen and Peddy, 1993). Rutherford and Williams classified the AVO responses of shale-gas sand interfaces (Rutherford and Williams, 1984) and such a case of a high impedance sand showing a polarity reversal with offset is termed a Class 1 anomaly. Under the revised classification of Young and LoPiccolo (2003) this is a Type 1 anomaly. The polarity reversal occurs at an offset of about 250 m and an incidence angle of about 35°.

PS synthetic seismograms

After successfully correlating the PP data and PP synthetic seismograms, we turned our attention to the PS data. Hampson-Russell's Geoview program was used to generate the PS synthetic for well 07-22-017-16W4M, shown in Figure 10. The shear sonic log was derived from the P sonic log, as discussed earlier and the wavelet was extracted from the PS seismic data. The polarity convention is that of the SEG, i.e., a positive peak represents an increase in acoustic impedance. This is opposite to the actual solution to the Zoeppritz equations for the PS reflection, which is increasingly negative with offset. The character tie here is very good for reflectors above about 800 m.

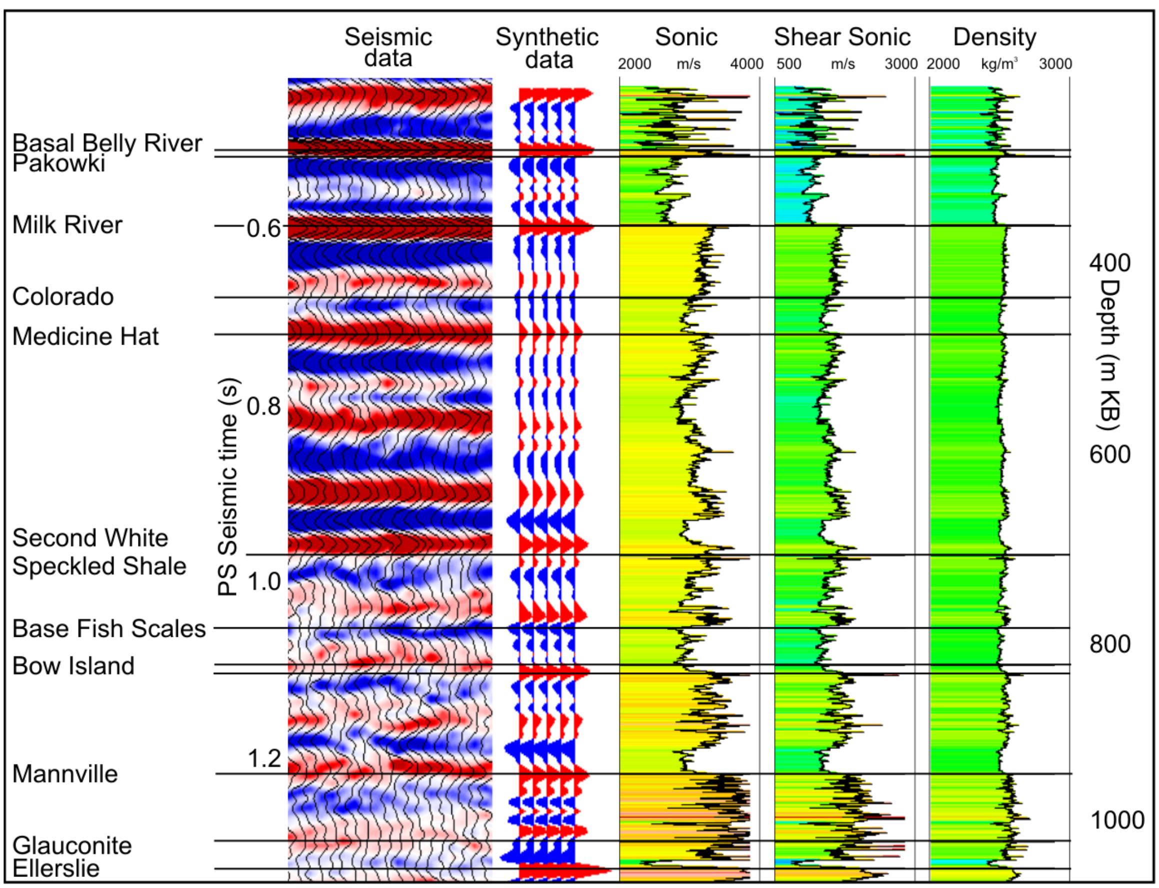

FIG. 10: Tie between PS seismic data and PS synthetic seismogram for well 07-22-017-16W4M.

SUMMARY

We created PP and PS synthetic seismograms to tie well formation tops to migrated PP and PS seismic data. The character tie at the top of the Milk River Formation between the PP seismic data processed with all offsets and the normal incidence synthetic seismogram is very poor. The Milk River is a high impedance sandstone which also has a lower Poisson's ratio than the overlying Pakowki shale. Thus the amplitude of the reflection coefficient is high at zero offset but decreases with increasing offset and even changes polarity. The synthetic seismogram stacked from a multiple offset synthetic gather matches the full-offset PP seismic data much better than does the normal incidence synthetic. The seismic character of the near-offset PP seismic data, with offsets only to 250 m, matches that of the normal incidence synthetic seismogram.

The PS data shows a good character match to the PS synthetic seismogram, which was created using a wavelet extracted from the PS data, and multiple offsets.

Tying the PP and PS data to synthetic seismograms now enables us to identify reflections, to register the two data sets, interpret them and create Vp/Vs maps.

ACKNOWLEDGEMENTS

We thank CaMI and the CREWES sponsors for their financial support. We also gratefully acknowledge support from NSERC (Natural Science and Engineering Research Council of Canada) through the grant CRDPJ 461179-13. We also appreciate the generous contribution by Halliburton/Landmark and Schlumberger of processing software. We acknowledge IHS for GeoSyn and CGG/Hampson-Russell Software Services for Geoview.

REFERENCES

Allen, J. L. and C. P. Peddy, 1993, Amplitude variation with offset: Gulf Coast case histories: Society of Exploration Geophysicists Geophysical development series, Vol. 4.

Aki, K. and P. G. Richards, 1980, Quantitative seismology: Theory and methods: W. H. Freeman and Co.

Castagna, J. P.; M. L. Batzle, and R. L. Eastwood, 1985, Relationships between compressional-wave and shear-wave velocities in clastic silicate rocks: Geophysics **50**: 571–581.

Isaac, J. H., and D. C. Lawton, 2014, Preparing for experimental CO_2 injection: Seismic data analysis: CREWES Research Report, Vol. 26.

Isaac, J. H., and D. C. Lawton, 2015, 3D3C seismic data at the Brooks experimental CO_2 injection site: CREWES Research Report, This volume.

Lawton, D. C., M. B. Bertram, K. L. Bertram, K. W. Hall and J. H. Isaac, 2014, A 3C-3D seismic survey at a field research station near Brooks, Alberta: CREWES Research Report, Vol. 26.

Margrave, G. F. and M. P. Lamoureux, 2002, Gabor deconvolution: CSEG Annual Convention Expanded Abstracts.

Rutherford, S. R. and R. H. Williams, 1989, Amplitude-versus-offset variations in gas sands: Geophysics, **54,** 680-688.

Young, R. A. and R. D. LoPiccolo, 2003, A comprehensive AVO classification: The Leading Edge, Vol. **22**, No. 10, 1030-1037.

Zoeppritz, K, 1919, Erdbebenwellen VIII B, Über reflexion und durchgang seismischer wellen durch unstetigkeitsflächen: Göttinger Nachrichten, **I**, 66-84.